NAR Genomics and Bioinformatics, 2025, **7**, lqaf052
https://doi.org/10.1093/nargab/lqaf052
Standard Article

OXFORD

SLAYER: a computational framework for identifying synthetic lethal interactions through integrated analysis of cancer dependencies

Ziv Cohen [1,2,†], Ekaterina Petrenko [2,†], Alma Sophia Barisaac [2], Enas R. Abu-Zhayia [2], Chen Yanovich-Ben-Uriel [2], Nabieh Ayoub [2], Dvir Aran [1,2,*]

[1]The Taub Faculty of Computer Science, Technion—Israel Institute of Technology, Haifa 3200003, Israel
[2]Faculty of Biology, Technion—Israel Institute of Technology, Haifa 3200003, Israel

[*]To whom correspondence should be addressed. Tel: +972 77 887 1909; Email: dviraran@technion.ac.il
[†]These authors contributed equally to this work.

Abstract

Synthetic lethality represents a promising therapeutic approach in precision oncology, yet systematic identification of clinically relevant synthetic lethal interactions remains challenging. Here, we present SLAYER (Synthetic Lethality AnalYsis for Enhanced taRgeted therapy), a computational framework that integrates cancer genomic data and genome-wide CRISPR knockout screens to identify potential synthetic lethal interactions. SLAYER employs parallel analytical approaches examining both direct mutation-dependency associations and pathway-mediated relationships across 1080 cancer cell lines. Our integrative method identified 682 putative interactions, which were refined to 148 high-confidence candidates through stringent filtering for effect size, druggability, and clinical prevalence. Systematic validation against protein interaction databases revealed an ∼14-fold enrichment of known associations among SLAYER predictions compared with random gene pairs. Through pathway-level analysis, we identified inhibition of the aryl hydrocarbon receptor (AhR) as potentially synthetically lethal with RB1 mutations in bladder cancer. Experimental studies demonstrated selective sensitivity to AhR inhibition in RB1-mutant versus wild-type bladder cancer cells, which probably operates through indirect pathway-mediated mechanisms rather than direct genetic interaction. In summary, by integrating mutation profiles, gene dependencies, and pathway relationships, our approach provides a resource for investigating genetic vulnerabilities across cancer types.

Introduction

Synthetic lethality represents a promising therapeutic strategy in precision oncology by exploiting genetic vulnerabilities exclusive to tumor cells [1]. This approach targets nononcogenic partners of mutated genes that cancers become dependent on, providing a means to selectively kill cancer cells while sparing normal tissues [2]. Notable examples of clinically relevant synthetic lethal interactions (SLIs) include PARP inhibitors in BRCA-mutated cancers [3] and WEE1 inhibitors in TP53-mutated tumors [4].

The systematic identification of SLIs has been pursued through various computational approaches. Early methods focused on evolutionary conservation of genetic interactions [5], while more recent approaches have leveraged cancer genomic data. For instance, computational frameworks like DAISY integrated somatic copy number alterations, gene expression, and short hairpin RNA (shRNA) data to predict SLIs [6]. Another approach, MiSL, analyzed mutation and copy number profiles to identify candidate synthetic lethal partners [1]. The advent of genome-wide CRISPR screens has enabled more direct approaches, as demonstrated by Chan *et al.* in identifying WRN as a synthetic lethal target in microsatellite unstable cancers [7]. Recent studies have highlighted the importance of pathway-level analysis in SLI prediction. For example, the ISLE framework incorporated pathway information to prioritize SLI candidates [1], while others have focused on specific pathway contexts, like DNA damage response genes [8]. However, most existing approaches either rely on direct gene–gene associations or treat pathways as discrete sets, potentially missing complex regulatory relationships that could influence synthetic lethality.

The Cancer Dependency Map (DepMap, https://depmap.org/portal/) provides comprehensive multi-omics data spanning over a thousand cancer cell lines, including genome-wide CRISPR–Cas9 knockout screens that measure cellular viability upon individual gene disruptions. While this resource has been leveraged for various analyses, systematic integration of mutation profiles, gene dependencies, and pathway-level information remains challenging. Previous studies using DepMap data have primarily focused on direct mutation-dependency associations through large-scale CRISPR screens [9] of pathway-level information.

Here, we present SLAYER (Synthetic Lethality AnalYsis for Enhanced taRgeted therapy), a computational framework that integrates multidimensional DepMap data to systematically identify associations between common cancer mutations and pathway dependencies. SLAYER builds upon previous approaches in three key ways: (i) it combines direct

Received: January 9, 2025. **Revised:** March 17, 2025. **Editorial Decision:** April 15, 2025. **Accepted:** April 16, 2025

mutation-dependency analysis with pathway-level investigation, (ii) it incorporates druggability and clinical relevance filters to prioritize actionable targets, and (iii) it enables exploration of indirect synthetic lethal relationships mediated through pathway rewiring. By intersecting mutation profiles with CRISPR gene essentiality patterns and pathway enrichment scores, our approach provides a systematic framework for nominating potential SLIs for experimental validation and therapeutic development.

Materials and methods

Data processing and quality control

This study utilized multi-omics data from the DepMap (https://depmap.org/portal/) portal, comprising 1080 cancer cell lines spanning 15 tissue types (DepMap 21Q1 release). We obtained gene expression profiles (RNA-seq), mutation annotations (DNA-seq), copy number alterations, and gene dependency scores from genome-scale CRISPR–Cas9 essentiality screens. To minimize confounding effects from genomic instability, we excluded 238 cell lines with excessive mutational burden (>100 putative damaging mutations). This filtering was applied across all tissue types, with varying exclusion rates depending on the typical mutation burden of each cancer type (Supplementary Table S1). We focused on 15 cancer types that had sufficient cell line representation (≥25 cell lines after filtering) and could be matched with TCGA data.

Driver gene-oriented analysis

The identification of driver genes began with characterization of nonsilent mutations (missense, nonsense, frameshift, or splice site) across the cell line panel. We defined recurrent mutations as those occurring at ≥2.5% frequency within specific cancer types. For each identified gene, we stratified cell lines into mutant and wild-type groups. We then calculated the delta dependency (DD) score between groups as

$$DD_{g,dg} = \overline{dependency_g \text{ in } WT_{dg}} - \overline{dependency_g \text{ in } MUT_{dg}} \quad (1)$$

where g represents the gene being tested and dg represents the driver gene. The term "dependency" refers to the gene essentiality scores derived from the DepMap CRISPR–Cas9 knockout screens, which quantify the impact of gene knockout on cell viability. These scores range from −1 (most essential) to 1 (least essential), with scores below ∼−0.5 typically indicating genes that are essential for cell survival. The overbar notation represents the mean dependency score across all cell lines in the respective group (wild-type or mutant for the driver gene). Statistical significance was assessed using two-sample t-tests with Benjamini–Hochberg correction for multiple testing.

Pathway enrichment-oriented analysis

Our pathway-level analysis framework incorporated 189 canonical oncogenic pathway signatures from the MSigDB C6 collection. We specifically selected this collection of oncogenic signatures because these gene sets directly capture transcriptional states associated with cancer-relevant signaling events. Unlike general biological pathways (such as those from KEGG or Reactome), these signatures represent experimentally derived gene expression patterns associated with oncogenic activation or tumor suppressor loss, making them particularly well suited for identifying synthetic lethal relationships in cancer.

We quantified pathway activity using single-sample gene set enrichment analysis and normalized enrichment scores across cell lines. To calculate the pathway score for each potential synthetic lethal pair, we implemented a two-tiered approach. First, we identified pathways potentially related to the driver gene by searching for the driver gene name within pathway annotations. For gene pairs where driver-related pathways were identified, we calculated the maximum absolute correlation between the partner gene's dependency profile and the enrichment scores of these driver-specific pathways.

These correlation-based relationships were then integrated into a weighted bipartite graph connecting genes and pathways, with edge weights determined by correlation coefficients. This network representation enabled visualization and exploration of the complex relationships between genetic alterations, pathway activities, and cellular dependencies. Edge weights in the network were determined by correlation coefficients, with edges filtered using an absolute correlation threshold of 0.5. The network visualization employed a sigmoid-based transparency function:

$$\sigma(w) = 1 - \frac{1}{1 + e^{20(|w|-0.6)}}. \quad (2)$$

To identify potential pathway-mediated relationships, we implemented a breadth-first search algorithm to discover connecting paths between driver gene mutations, gene dependencies, and intermediate pathway nodes. Path scoring incorporated both edge weights and directionality of correlations.

Candidate SLI prioritization

The prioritization of SLIs followed a systematic framework integrating multiple evidence sources. Statistical significance requirements included adjusted P-value <.05 and DD > 0.2, and additionally pathway score >0.2. For driver gene identification, we initially identified genes with mutation frequency ≥2.5% across cell lines, but additionally required that these genes must be classified as known cancer genes in at least one established database (COSMIC Cancer Gene Census, OncoKB, or IntOGen) to ensure focus on true cancer drivers rather than passenger mutations. Clinical relevance was further assessed through TCGA mutation frequency data from cBioPortal, requiring >15% frequency in the relevant cancer type. Therapeutic potential was evaluated using the DepMap PRISM repurposing database to identify druggable target genes.

We validated predicted interactions through comparison with STRING database version 12.0, considering all evidence types with a minimum combined score threshold of 0.4. While STRING does not directly catalog synthetic lethal relationships, protein–protein interactions and functional associations have been shown to be enriched among synthetic lethal gene pairs [6, 7]. Statistical analyses were performed using R (version 4.1.0), with multiple testing correction applied within each cancer type.

All code and detailed documentation are available at https://github.com/zivc888/SLICE. A Shiny application is publicly available at https://dviraran.shinyapps.io/SLAYER and provides an accessible way to interact with our results, examine specific driver genes or cancer types of interest, and visualize the supporting evidence for predicted SLIs.

Experimental validation of the SLI between RB1 and AhR in bladder cancer

Cell lines and cell culture

T24 and 5637 cell lines were grown in RPMI-1640 medium (Gibco) supplemented with 10% heat-inactivated fetal bovine serum (FBS), 2 mM L-glutamine, and 100 mg/ml penicillin/streptomycin. RPE1-hTERT wild-type and p53 −/− cell lines were grown in Dulbecco's modified Eagle's medium (Gibco) supplemented with 10% heat-inactivated FBS, 2 mM L-glutamine, and 100 mg/ml penicillin/streptomycin.

Lentiviral transduction

Lentiviral particles were generated by co-transfecting HEK293T cells plated in 10-cm plates with 1.64 pmol target vector, together with 1.3 pmol psPAX2 (Addgene, #12260) and 0.72 pmol pMD2.G (Addgene, #12259) using 3:1 μg Polyethylenimine (PEI) to μg DNA ratio. Media containing the viral particles was collected 48 h post-transfection and filtered with 0.45-μm filters. The indicated cell lines were transduced with the lentiviral particles in the presence of 10 μg/ml polybrene (Sigma–Aldrich, H9268). At 48 h post-infection, transduced cells were selected using the appropriate antibiotics.

shRNA knockdown

shRNA oligonucleotides directed against RB1 were annealed and cloned into pLKO-puro lentiviral vector (Addgene, #10878) digested with EcoRI and AgeI. Lentiviral particles were generated as described above and used to transduce T24 cells, followed by selection with 1 μg/ml puromycin (Invivogen, #ant-pr) for 3 days. Cells were maintained in complete medium in the presence of 0.6 μg/ml puromycin. Gene expression knockdown was validated by reverse transcription-quantitative PCR (RT-qPCR). The shRNA and qPCR primer sequences used in this study are included in Supplementary Table S2.

RNA isolation and qPCR

Total RNA was isolated from cells using the TRIzol reagent according to the manufacturer's instructions (Sigma). A total of 1 μg RNA was used for complementary DNA synthesis using the qScript cDNA Synthesis Kit (Quanta) with random primers. Real-time qPCR for measuring messenger RNA levels was performed using Step-One-Plus Real-Time PCR System (Applied Biosystems) and the Fast SYBR Green Master Mix (Applied Biosystems) with three technical repeats for each PCR. Data analysis and quantification were performed using StepOne software version 2.2 supplied by Applied Biosystems. Primer sequences used for qPCR are included in Supplementary Table S2.

AhR inhibitor

BAY-2416964 was purchased from Selleckchem.

Short-term growth delay assay

For determining drug sensitivity, cells were seeded in 96-well plates in duplicates at a density of 3000–7500 cells per well. Then, 24 h post-seeding, BAY-2416964 was added at the indicated concentrations. Cell viability was measured at the indicated timepoints using the CellTiter 96® AQueous One Solution Cell Proliferation Assay (Promega) following the manufacturer's protocol, and absorbance was measured using Epoch Microplate Spectrophotometer (BioTek). Cell viability was normalized to the viability of untreated cells.

Results

The SLAYER computational framework integrates multidimensional data from the DepMap resource to systematically identify SLIs across cancer types. Our analysis included 1080 cancer cell lines with complete genomic and transcriptomic profiles alongside CRISPR–Cas9 gene essentiality screens. For our initial analysis, we selected genes with mutations present in at least 2.5% of cell lines within each cancer type, ensuring sufficient statistical power when comparing mutant and wild-type groups. From this set, we identified putative driver genes by requiring presence in established cancer databases, ultimately yielding 79 cancer-associated driver genes across the 15 cancer types analyzed.

Using the DepMap CRISPR–Cas9 knockout viability data, we calculated gene-specific dependency scores and their associations with driver gene mutations to identify potential SLIs through complementary analytical approaches (Fig. 1). Our integrated methodology combines two analytical dimensions: a direct mutation-dependency analysis examining the immediate impact of driver mutations on gene essentiality, and a pathway-oriented analysis that captures broader cellular context using experimentally-derived oncogenic signatures from MSigDB (see the "Materials and methods" section). This integrated analysis yielded 682 statistically significant potential SLIs (adjusted P-value $<.05$) with both DD scores and pathway enrichment scores exceeding 0.2.

We then applied stringent filtering criteria to prioritize clinically actionable candidates. First, we filtered for partner genes that are possible therapeutic targets by cross-referencing against the DepMap PRISM repurposing data, retaining only SLIs where the partner gene is inhibitable by an existing drug or compound. Next, we filtered for SLIs involving driver gene mutations with a population frequency >15% based on TCGA data. This ensures the SLIs are applicable to a sufficiently broad patient population. After this multistep filtering process focused on statistical significance, effect size, druggability, and clinical relevance, we identified a refined set of 148 high-confidence, actionable potential SLIs for further prioritization and experimental validation (Fig. 2 and Supplementary Table S3). The top-scoring SLIs from this analysis are presented in Table 1, showing strong statistical significance and high effect sizes across multiple cancer types.

We analyzed our list of 148 putative SLIs and identified numerous pairs with strong mechanistic coherence, including several that have been previously experimentally validated. Among the 55 pairs involving TP53 as the driver gene, the TP53–TXNRD1 interaction (in liver cancer, DD = 0.94, pathway score = 0.55) showed the strongest dependency effects. This interaction has a strong mechanistic basis, as p53-deficient cancer cells exhibit increased reliance on redox management systems. We also identified TP53–TXN in the same pathway, suggesting that the entire thioredoxin system becomes critical when p53 is lost. Studies demonstrate that simultaneously disabling glutathione and thioredoxin antioxidant pathways is lethal to cancer cells, making these compelling targets for p53-mutant tumors [10]. The well-studied TP53–CHEK1 interaction (in melanoma, DD = 0.49,

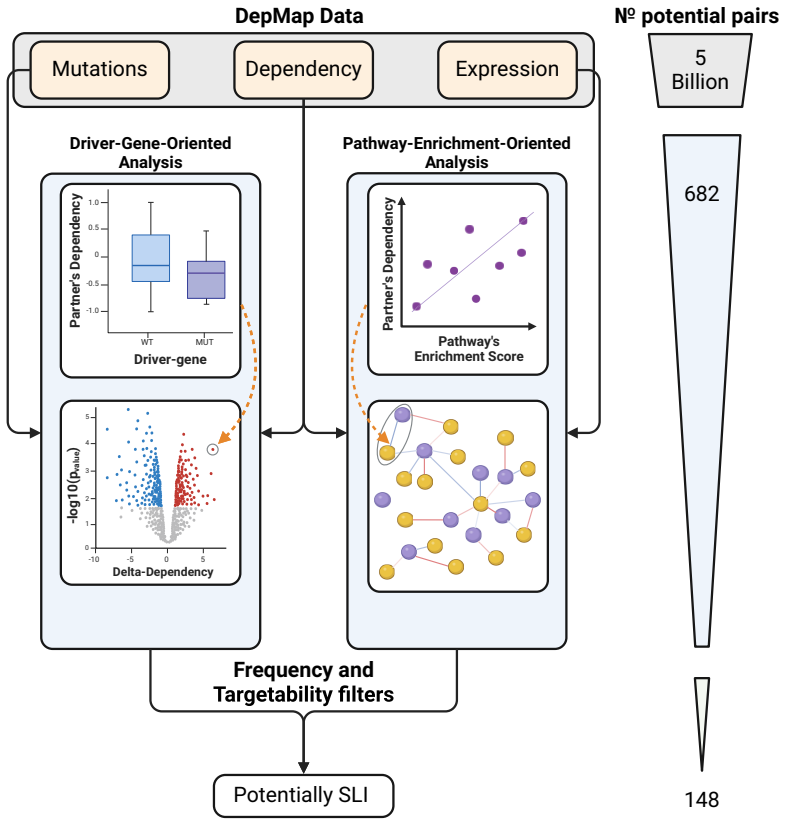

Figure 1. Schematic overview of the SLAYER methodology. Data from the DepMap portal, including mutations, gene dependencies, and expression profiles across 1080 cancer cell lines, were integrated using two complementary approaches: (i) a driver gene-oriented analysis associating gene dependencies with driver mutations, and (ii) a pathway enrichment-oriented analysis connecting gene dependencies with mutation-associated pathway activities. Putative SLIs were identified by requiring statistical significance and effect size thresholds (scores >0.2) in both analytical approaches. These candidates were further filtered based on the driver gene mutation frequency in the patient population and druggability of the partner gene. From an initial ∼5 billion possible gene pairs, 682 statistically significant SLI candidates were identified, which were then refined to a set of 148 high-confidence, actionable SLIs based on effect size, targetability, and clinical relevance filters.

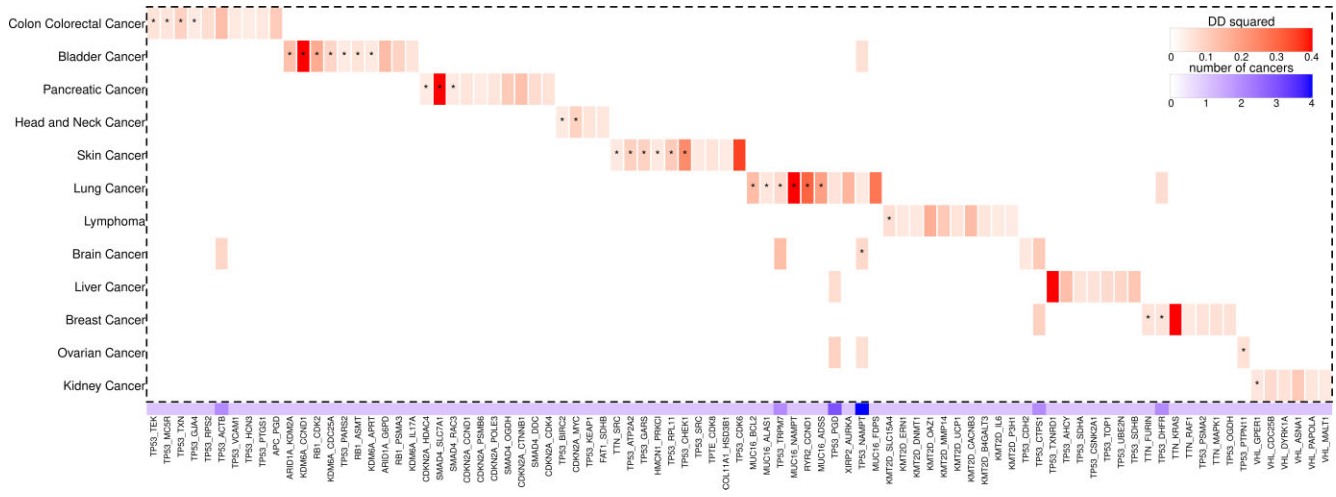

Figure 2. Potential SLIs across cancer types. The heatmap displays the top 10 most significant SLIs identified for each cancer type in the analysis. The red color scale corresponds to the DD score, representing the difference in gene essentiality between the mutant and wild-type groups. The blue bar at the bottom indicates the number of cancer types where the SLI was determined as statistically significant. SLIs with *P*-value <.01 are marked with an asterisk.

Table 1. Top potential SLIs

Pair	Cancer type	Driver's freq	*P*-value	DD	Pathway	Validation
TP53–TXNRD1	Liver cancer	30.8%	.014	0.94	0.58	Yes
KDM6A–CCND1	Bladder cancer	25.2%	.004	0.76	0.54	Yes
SMAD4–SLC7A1	Pancreatic cancer	22.4%	.003	0.68	0.44	No
MUC16–FDPS	Lung cancer	40.7%	.013	0.52	0.50	No
RB1–PAICS	Bladder cancer	16.9%	.049	0.48	0.52	No
RYR2–CCND1	Lung cancer	38.9%	.008	0.55	0.41	No
RB1–AHR	Bladder cancer	16.9%	.019	0.46	0.44	Yes
RB1–CDK2	Bladder cancer	16.9%	.005	0.42	0.41	Yes
KMT2D–OAZ1	Lymphoma	29.8%	.018	0.41	0.42	No

Top SLIs from our analysis are presented, including DD scores and pathway scores. Validation indicates interactions with experimental evidence in STRING-db. SLIs presented have DD > 0.4 and pathway score >0.4, ordered by the sum of both.

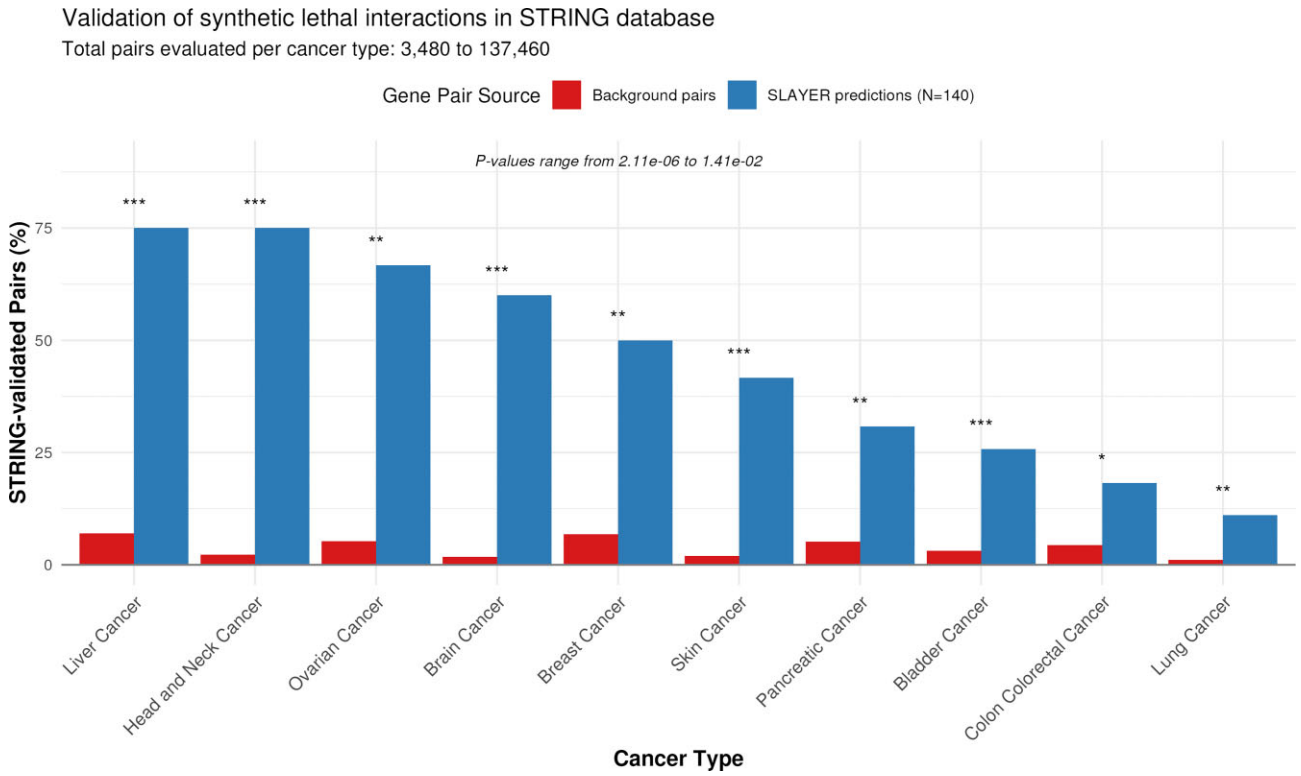

Figure 3. Validation of predicted SLIs against STRING-db database. Bar plots show the percentage of gene pairs from the SLAYER analysis that exhibited evidence of interaction or co-occurrence in the STRING-db database, which integrates known and predicted protein associations from multiple sources. The blue bars represent the percentages for the 148 high-confidence SLIs identified by SLAYER, while the red bars indicate the background percentages when analyzing all possible pairwise combinations of driver genes and genes across the different cancer types. Fisher's exact test revealed highly significant enrichment in multiple cancer types ($P < 1e{-}5$ for bladder, liver, and skin cancer), with all cancer types showing significant enrichment ($P < .05$).

pathway score = 0.36) has been experimentally validated as synthetically lethal [11], although subsequent studies have raised concerns about its clinical utility [12, 13]. Intriguingly, TP53–NAMPT appeared as a potential SLI across four different cancer types (brain, ovarian, bladder, and lung), suggesting NAMPT as a broadly applicable target in p53-mutated cancers. This aligns with studies showing that TP53-deficient cells rely more heavily on NAD+ metabolism, making them particularly vulnerable to NAMPT inhibition [14].

For the 15 RB1-driven pairs, the RB1–CDK2 interaction in bladder cancer (DD = 0.42, pathway score = 0.41) is supported by strong evidence. Studies have shown that RB1-deficient cells have unrestrained E2F activity, making Cyclin E/CDK2 crucial for S-phase progression. Loss of RB1 leads to upregulation of E2F target genes, causing cells to become "addicted" to CDK2 for continued cycling. Multiple experiments have demonstrated that knocking down or inhibiting CDK2 selectively killed cells with RB1 loss while sparing RB1-intact cells [15]. Among the nine CDKN2A pairs, the most significant was with CDK4 (DD = 0.25, pathway score = 0.44), a well-established relationship where loss of $p16^{INK4A}$ leads to hyperactivation of CDK4/6-Cyclin D, creating dependency on CDK4/6 activity. This forms the basis for treating p16-null cancers with CDK4/6 inhibitors, with clinical evidence showing ~50% of p16-null patients responded to palbociclib in trials [16]. We also identified CDKN2A–CCND1 as synthetically lethal, representing the same pathway and reinforcing the critical nature of this cell cycle vulnerability.

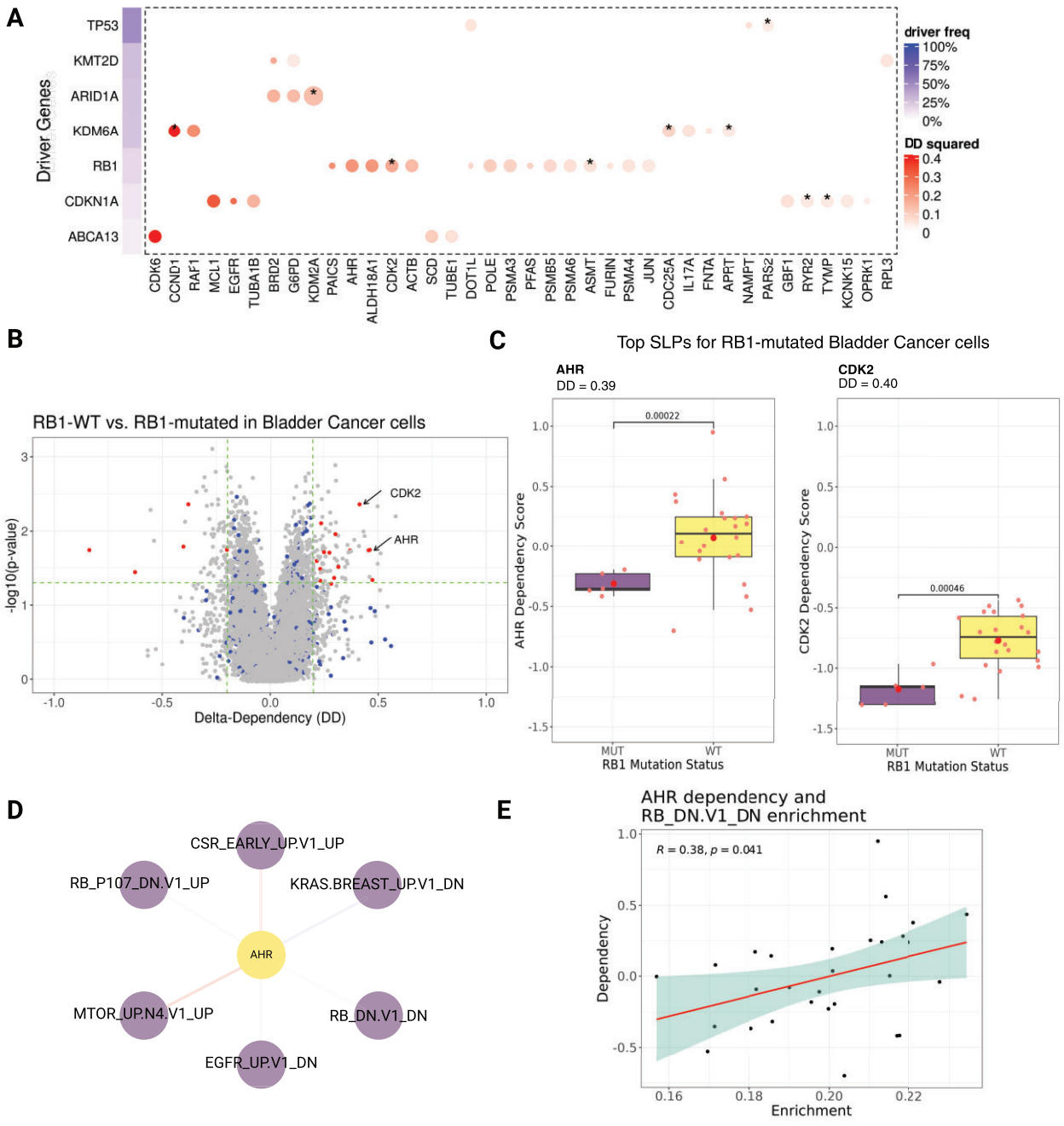

Figure 4. Potential SLIs in bladder cancer. (**A**) Heatmap depicting the top SLI pairs in bladder cancer, with redder colors indicating higher DD scores. Similar heatmaps for each of the cancer types are available in Supplementary Fig. S1. (**B**) Volcano plot showing all potential SLIs for the RB1 mutation, with AHR and CDK2 identified as the top-ranking candidates based on DD (*x*-axis) and statistical significance ($-\log_{10}$ *P*-value on *y*-axis). More examples in Supplementary Fig. S2. (**C**) Boxplots illustrating the separation in gene dependency scores between RB1 wild-type and RB1 mutant bladder cancer cell lines for the AHR and CDK2. (**D**) Dependency network for AHR in bladder cancer, highlighting edges that connect these genes to RB1-associated pathways. (**E**) Correlation plot between the dependency scores of AHR and the enrichment of RB1-related pathway across the cell lines.

To systematically validate our predictions, we compared them against STRING-db, a comprehensive database integrating known and predicted protein–protein interactions. We found that 42 of 148 (28.4%) high-confidence predictions showed STRING-db support compared with only 1.0%–7.0% for random pairs of driver genes and partner genes (Fig. 3). This striking ~14-fold enrichment highlights the ability of our integrated analytical approach to capture biologically meaningful relationships.

In bladder cancer, our analysis focused on 46 cell lines harboring 7 recurrent driver mutations (Fig. 4A; similar analyses for other cancer types are available in Supplementary Figs S1–S2). The top SLIs implicated KDM6A mutant sensitivity to CCND1 knockout and several potential vulnerabilities in RB1 mutant tumors (Fig. 4B and C). RB1 mutations were observed in 18.9% of the bladder cancer cohort, consistent with 16.8% prevalence in TCGA patient samples. Pathway enrichment analysis confirmed associations between AHR knockout de-

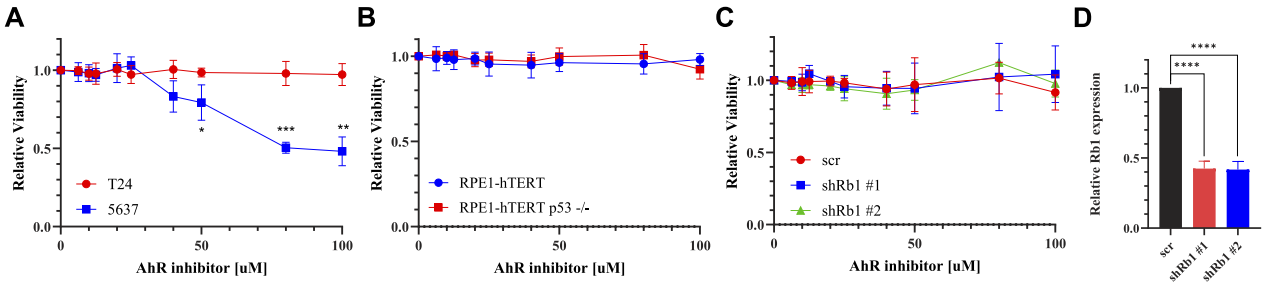

Figure 5. Synthetic lethality between RB1 and aryl hydrocarbon receptor (AhR) in bladder cancer.(**A**) Short-term cell viability assay in T24 and 5637 cells treated with increasing concentrations of BAY-2416964. Cell viability was measured 24 h after drug treatment. Data are presented as mean ± s.d. ($n = 3$). $*P < .05$; $**P < .01$; $***P < .001$. (**B**) Short-term cell viability assay in p53 wild-type (WT) and p53 null RPE1-hTERT cells treated with increasing concentrations of BAY-2416964. Cell viability was measured 24 h after drug treatment. Data are presented as mean ± s.d. ($n = 3$). (**C**) Short-term cell viability assay in T24 cells expressing either scramble shRNA or shRNA targeting Rb1 and treated with increasing concentrations of BAY-2416964. Cell viability was measured 72 h after drug treatment. Data are presented as mean ± s.d. ($n = 3$). (**D**) Quantitative RT-qPCR analysis of Rb1 knockdown in indicated T24 cell lines. $****P < .0001$.

pendency and RB1-related signatures, prompting experimental validation of this SLI (Fig. 4D and E).

To provide preliminary experimental support for this computational prediction, we examined cellular responses to the AHR inhibitor BAY-2416964 in bladder cancer cell lines. The RB1-mutant cell line 5637 exhibited markedly increased sensitivity to AHR inhibition compared with the RB1-wild-type T24 line (Fig. 5A). Importantly, BAY-2416964 treatment showed no significant impact on noncancerous RPE cells, supporting the context-specific nature of this SLI (Fig. 5B). We then tested whether acute RB1 loss would sensitize cells to AHR inhibition by depleting RB1 in T24 cells using shRNA. Despite achieving significant RB1 knockdown, RB1-depleted T24 cells showed no enhanced sensitivity to BAY-2416964 (Fig. 5C and D). This suggests the synthetic lethality may arise through indirect mechanisms involving broader cellular rewiring in the context of established RB1 mutations rather than acute RB1 loss.

Discussion

In this study, we developed SLAYER, an integrated computational framework that systematically mines multi-omics data from the DepMap cancer cell line resource to nominate and prioritize SLIs associated with recurrent driver mutations across cancer types. Our approach combines complementary techniques examining mutational patterns alongside CRISPR gene essentiality profiles and pathway enrichment signatures. This integration enables detection of both direct genetic dependencies and indirect relationships mediated through cellular networks, providing a more comprehensive view of potential therapeutic vulnerabilities.

The systematic validation of SLAYER predictions against STRING database interactions demonstrates the biological relevance of our computational approach. The ∼14-fold enrichment of known protein associations among predicted synthetic lethal pairs suggests our methodology effectively captures meaningful cellular relationships rather than statistical artifacts. This enrichment is particularly noteworthy given that STRING interactions represent a conservative validation set, as many genuine synthetic lethal relationships may involve genes without direct physical interactions.

Among the high-confidence predictions, the synthetic lethal relationship between RB1 mutations and AHR inhibition in bladder cancer emerged as particularly promising. Our experimental studies confirmed increased sensitivity to AHR inhibition in RB1-mutant versus WT bladder cancer cells, while sparing noncancerous cells. However, the lack of sensitization in RB1-depleted cells suggests this synthetic lethality may arise through indirect mechanisms involving broader cellular adaptations to established RB1 loss. We hypothesize that long-term RB1 deficiency leads to compensatory rewiring of cellular pathways and epigenetic reprogramming that creates a dependency on AHR function which is not immediately established upon acute RB1 depletion.

The apparent indirectness of the RB1–AHR relationship also highlights the value of our pathway-oriented analytical approach. Traditional methods focused solely on direct genetic interactions might miss such context-dependent vulnerabilities. By incorporating pathway-level information and allowing for network-mediated relationships, SLAYER can potentially identify therapeutic opportunities that emerge from complex cellular rewiring during tumor evolution. This capability is especially relevant for tumor suppressors like RB1, where acute gene loss may not fully recapitulate the cellular state that develops through prolonged adaptation to mutation.

However, we acknowledge that genetic background differences between the cell lines used in our study may contribute to the observed synthetic lethality beyond the RB1 mutation status alone. The complex mutational landscapes of cancer cell lines can harbor additional genetic alterations that interact with both RB1 and AHR pathways, potentially confounding the interpretation of direct synthetic lethal relationships. Additional studies with isogenic cell line pairs and broader panels of cell lines would be necessary to fully delineate the mechanisms and genetic contexts in which the RB1–AhR synthetic lethality operates.

Several limitations of our study warrant discussion. First, while our computational predictions showed strong statistical enrichment for known interactions in STRING-db, broader validation against experimental synthetic lethal datasets [17–19] would strengthen confidence in our predictions. Second, direct comparison with other computational prediction methods would help establish SLAYER's relative performance. These important validations were beyond the scope of this study but represent valuable directions for future work.

Despite these limitations, SLAYER represents a valuable framework for systematic exploration of SLIs in cancer. The successful prediction and preliminary validation of RB1–AHR synthetic lethality demonstrates the potential for computational approaches to guide therapeutic discovery. Our comprehensive characterization of potential SLIs across multiple cancer types provides a rich resource for future investigation. The pathway-oriented analytical approach may be particularly valuable for understanding complex dependencies that emerge through cellular adaptation to oncogenic mutations.

Looking forward, several promising directions emerge for extending this work. Integration of additional data modalities, such as metabolomic or proteomic profiles, could provide deeper mechanistic insights. Incorporation of patient-derived models or clinical response data could help bridge the gap between cell line predictions and therapeutic applications. Finally, adaptation of our framework to analyze temporal dynamics or cellular plasticity might reveal context-dependent synthetic lethal relationships that could inform treatment strategies.

In conclusion, SLAYER provides a systematic approach for discovering potential SLIs with direct therapeutic relevance. While additional validation studies are warranted, our computational framework offers a valuable resource for prioritizing experimental investigation of cancer-specific vulnerabilities. The identification of AHR inhibition as a potential therapeutic strategy in RB1-mutant bladder cancer exemplifies the capacity of integrated computational analysis to reveal promising therapeutic opportunities.

Acknowledgements

We thank Hinanit Koltai for generously sharing cell lines. We thank the Aran Lab members for helpful comments.

Author contributions: Conceptualization: D.A. Methodology:Z.C., D.A. Software: Z.C., E.P. Formal Analysis: Z.C., E.P., D.A. Investigation: Z.C., E.P., C.Y.-B.-U., A.S.B., E.R.A.-Z., N.A., D.A., Resources: D.A., N.A Data Curation: Z.C., E.P. Writing - Original Draft: Z.C., E.P., D.A. Writing - Review & Editing: E.P., D.A. Visualization: Z.C., E.P. Supervision: D.A., N.A. Project Administration: D.A. Funding Acquisition: D.A., N.A. Z.C. and E.P. contributed equally to this work. All authors reviewed the results and approved the final version of the manuscript.

Supplementary data

Supplementary data is available at NAR Genomics & Bioinformatics online.

Conflict of interest

D.A. reports consulting fees from Carelon Digital Platforms.

Funding

D.A. is supported by the Azrieli Faculty Fellowship. A.S.B. is supported by Joan and Irwin Jacobs fellowship. N.A. is supported by the Neubauer Family Foundation. Research in the Aran lab is supported by grant from the Israel Science Foundation (1543/21). Research in the Ayoub lab is supported by grants from the Israel Science Foundation (2511/19) and Israel Cancer Research Fund (22-110-PG).

Data availability

All data used in this study are publicly available at the DepMap portal. The code developed in this study is available at https://github.com/zivc888/SLICE and https://doi.org/10.6084/m9.figshare.28805912.v1.

References

1. Lee JS, Das A, Jerby-Arnon L *et al.* Harnessing synthetic lethality to predict the response to cancer treatment. *Nat Commun* 2018;**9**:2546. https://doi.org/10.1038/s41467-018-04647-1
2. Hartman JL, Garvik B, Hartwell L. Principles for the buffering of genetic variation. *Science* 2001;**291**:1001–4. https://doi.org/10.1126/science.1056072
3. Lord CJ, Ashworth A. PARP inhibitors: synthetic lethality in the clinic. *Science* 2017;**355**:1152–58. https://doi.org/10.1126/science.aam7344
4. Hu J, Cao J, Topatana W *et al.* Targeting mutant p53 for cancer therapy: direct and indirect strategies. *J Hematol Oncol* 2021;**14**:157. https://doi.org/10.1186/s13045-021-01169-0
5. Boone C, Bussey H, Andrews BJ. Exploring genetic interactions and networks with yeast. *Nat Rev Genet* 2007;**8**:437–49. https://doi.org/10.1038/nrg2085
6. Jerby-Arnon L, Pfetzer N, Waldman YY *et al.* Predicting cancer-specific vulnerability via data-driven detection of synthetic lethality. *Cell* 2014;**158**:1199–209. https://doi.org/10.1016/j.cell.2014.07.027
7. Chan EM, Shibue T, McFarland JM *et al.* WRN helicase is a synthetic lethal target in microsatellite unstable cancers. *Nature* 2019;**568**:551–6. https://doi.org/10.1038/s41586-019-1102-x
8. Benfatto S, Serçin z, Dejure FR *et al.* Uncovering cancer vulnerabilities by machine learning prediction of synthetic lethality. *Mol Cancer* 2021;**20**:111. https://doi.org/10.1186/s12943-021-01405-8
9. Behan FM, Iorio F, Picco G *et al.* Prioritization of cancer therapeutic targets using CRISPR–Cas9 screens. *Nature* 2019;**568**:511–6.https://doi.org/10.1038/s41586-019-1103-9
10. Haffo L, Lu J, Bykov VJN *et al.* Inhibition of the glutaredoxin and thioredoxin systems and ribonucleotide reductase by mutant p53-targeting compound APR-246. *Sci Rep* 2018;**8**:12671.https://doi.org/10.1038/s41598-018-31048-7
11. Chen Z, Xiao Z, Gu Wz *et al.* Selective Chk1 inhibitors differentially sensitize p53-deficient cancer cells to cancer therapeutics. *Int J Cancer* 2006;**119**:2784–94. https://doi.org/10.1002/ijc.22198
12. Zenvirt S, Kravchenko-Balasha N, Levitzki A. Status of p53 in human cancer cells does not predict efficacy of CHK1 kinase inhibitors combined with chemotherapeutic agents. *Oncogene* 2010;**29**:6149–59. https://doi.org/10.1038/onc.2010.343
13. Goto H, Izawa I, Li P *et al.* Novel regulation of checkpoint kinase 1: is checkpoint kinase 1 a good candidate for anti-cancer therapy? *Cancer Sci* 2012;**103**:1195–200.
14. Cerna D, Li H, Flaherty S *et al.* Inhibition of nicotinamide phosphoribosyltransferase (NAMPT) activity by small molecule GMX1778 regulates reactive oxygen species (ROS)-mediated cytotoxicity in a p53- and nicotinic acid phosphoribosyltransferase1 (NAPRT1)-dependent manner. *J Biol Chem* 2012;**287**:22408–17.
15. Dick FA, Li SSC. Drugging RB1 deficiency: synthetic lethality with aurora kinases. *Cancer Disc* 2019;**9**:169–72. https://doi.org/10.1158/2159-8290.CD-18-1448
16. Gopalan PK, Villegas AG, Cao C *et al.* CDK4/6 inhibition stabilizes disease in patients with p16-null non-small cell lung

cancer and is synergistic with mTOR inhibition. *Oncotarget* 2018;**9**:37352–66. https://doi.org/10.18632/oncotarget.26424
17. Shen JP, Zhao D, Sasik R *et al.* Combinatorial CRISPR–Cas9 screens for *de novo* mapping of genetic interactions. *Nat Methods* 2017;**14**:573–6.
18. Horlbeck MA, Xu A, Wang M *et al.* Mapping the genetic landscape of human cells. *Cell* 2018;**174**:953–67.
19. Zhao J, Cheng F, Wang Y *et al.* Systematic prioritization of druggable mutations in ∼5000 genomes across 16 cancer types using a structural genomics-based approach. *Mol Cell Proteomics* 2016;**15**:642–56.

Received: January 9, 2025. **Revised:** March 17, 2025. **Editorial Decision:** April 15, 2025. **Accepted:** April 16, 2025